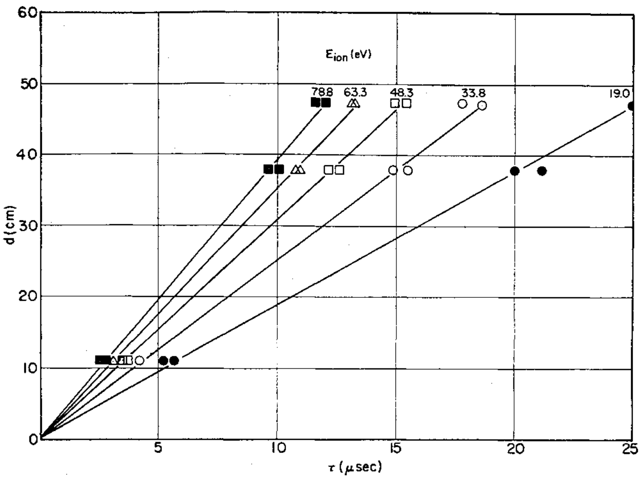

Fig. 3 Transmitting distance as function of laspse time for different plasma drift velocities.

In Fig. 3, the transmitting distances are plotted as functions of the lapse times for different velocities. The strict proportionality of the distance vs time proves that we have no noticeable influence of plasma sheath effects on the acoustic wave velocity ν_w given by the slope. Further, it was found that the mentioned variation of the plasma density did not affect the lapse time.

The acoustic wave velocities ν_w determined from the time-of-flight data shown in Fig. 3, are compared, in Fig. 4, with the ion drift velocities ν_d obtained from the electrostatic energy analyzer. The agreement of ν_w with ν_d indicates that the propagation velocity of the acoustic waves has a negligible effect in this range of velocities; i.e., $\nu_p \ll \nu_d$.

The described ion acoustic wave technique is particularly desirable for plasma drift velocity measurements in that it has been proved, within the limits of this experiment, to be independent of plasma density, does not depend on ion mass or charge, but rather, requires only the knowledge of the probe separation and wave lapse time. In addition to drift velocity measurements in the plasma wind tunnel, it is the intent of the authors to apply the technique, in a further stage of development, to the determination of orbital speeds of space vehicles in the ionosphere. Further investigations will be directed towards extension of the plasma parameter limits and the influence of the electron temperature on the propagation process.

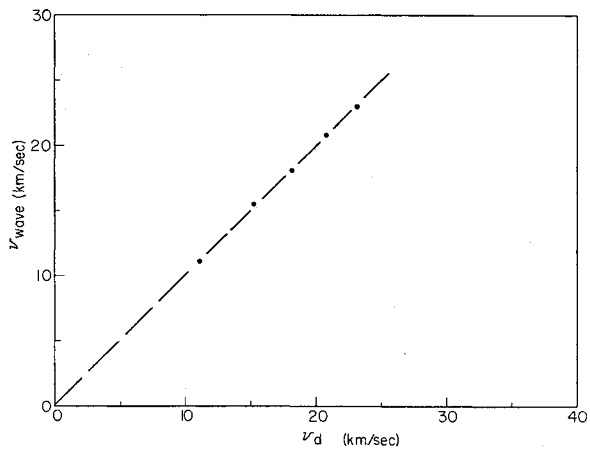

Fig. 4 Comparison of ion drift velocity ν_d and wave transmission velocity ν_w.

References

[1] Spitzer, L., Jr., *Physics of Fully Ionized Gases*, Interscience, New York, 1962.

[2] Alexeff, I., Jones, W. D., and Montgomery, D., "Effects of Electron-Temperature Variation on Ion Acoustic Waves," *The Physics of Fluids*, Vol. 11, 1968, pp. 167–173.

[3] Hall, D. F., Kemp, R. F., and Sellen, J. M., Jr., "Generation and Characteristics of Plasma Wind-Tunnel Streams," *AIAA Journal*, Vol. 3, No. 8, Aug. 1965, pp. 1490–1497.

Nonlinear Beam Vibration with Variable Axial Boundary Restraint

B. G. Wrenn*

Lockheed Missiles and Space Company, Sunnyvale, Calif.

AND

J. Mayers†

Stanford University, Stanford, Calif.

Nomenclature

A = cross-sectional area of beam
D_Q = transverse shearing stiffness of beam, $\gamma = Q/D_Q$
E = Young's modulus
g = time-dependent lateral displacement amplitude function
h = time-dependent axial displacement amplitude function
i = time-dependent shear angle amplitude function
I = cross-sectional moment of inertia of beam
k_D = spring constant representing axial restraint
K = nondimensional spring constant parameter, $K = k_D l/AE$
K_1 = complete elliptic integral of the first kind
l = length of beam
Q = shearing force
r = radius of gyration of the cross section, $r = (I/A)^{1/2}$
t = time
u = axial displacement of beam midsurface
w = lateral displacement of beam midsurface
w_{MAX} = maximum lateral displacement
x,z = axial and lateral coordinates
α = nondimensional function of displacement, $\alpha = (g_{MAX}/r)$: (for example with hinged ends, $g_{MAX} = w_{MAX}$; for example with clamped ends, $g_{MAX} = w_{MAX}/2$)
γ = shearing strain in beam
ω_n = actual frequency of nth mode lateral vibration
ω_0 = frequency as given by elementary theory for the nth mode

An investigation[1] was undertaken to establish simultaneously the effects of transverse shear, rotatory inertia, and variable midplane stretching on the lateral vibration behavior of solid and sandwich beams. This investigation was the forerunner of a more extensive program aimed at establishing frequency prediction capability for internal structural members of aerospace vehicles. These structural members reflect the use of nonclassical boundary restraints.

After the study conducted in Ref. 1, other investigations[2,3] appeared that dealt, in different theoretical fashions, with the limiting case of infinite axial restraint but yielded identical or essentially identical results. It is felt that the method of analysis employed in Ref. 1 is more easily adaptable to real structures and provides a more direct approach to the prob-

Received April 27, 1970; revision received June 1, 1970. Work supported by the U.S. Army Aviation Materiel Laboratories Contract DA44-177-AMC-115(t). A portion of the work reported herein was submitted by B. G. Wrenn in partial fulfillment of the requirements for the degree of Doctor of Philosophy, Stanford University, Stanford, Calif.

* Group Engineer, Aeromechanics Department, Space Systems Division; formerly Research Assistant, Department of Aeronautics and Astronautics, Stanford University. Member AIAA.

† Professor and Vice-Chairman, Department of Aeronautics and Astronautics. Associate Fellow AIAA.

lem. This Note will elaborate on the method of Ref. 1 as well as comment on Refs. 2 and 3. It should be further mentioned that the theoretical results are in good agreement with experiments recently conducted by Ray and Bert.[4] Reference 2 reflects the explicit assumption of harmonic vibratory motion. This assumption is not rigorously correct, as may be ascertained from Refs. 5–9. Unless allowance is made for the occurrence of nonharmonic motion, it cannot be assumed that approximate solutions, based on the assumption of harmonic motion, will lead to accurate results for unconventional structures and boundary conditions other than classical hinged support. Reference 3 employs a perturbation technique to derive approximate frequency relations for uniform beams with various end conditions. The spatial variations of the mode shapes and the evaluation of various integral expressions are taken from Refs. 10 and 11. This represents a nice solution for the problem posed but could present difficulties for different geometries and different boundary conditions since the mode shapes and the integral expressions would have to be generated.

The amount of midplane stretching will depend on the manner in which the ends of the beam are actually restrained. In an attempt to assess this nonlinear effect, the variable end restraint is initially assumed to be represented by a linear spring, unstretched under zero lateral deflection. It is believed that Ref. 1 is the first to consider arbitrary axial restraint. Previous investigations that considered the vibrations of beams with complete axial restraint are given in the literature.[2,3,5–9,12] The governing differential equations and the attendant boundary conditions are developed[1] utilizing a variational procedure. In addition, Ref. 1 presents two approximate solutions. These examples are presented here to illustrate the technique. For a uniform homogeneous beam, functions representing the degrees of freedom which satisfy the geometric boundary conditions, but are arbitrary in time, may be taken in the form

$$w = g(t)\sin(n\pi x/l),\ u = h(t)[C_1x + C_2\sin(2n\pi x/l)] \qquad (1)$$
$$\gamma = i(t)\cos(n\pi x/l)$$

where C_1 and C_2 are constants. Substitution of Eq. (1) into the potential energy and application of Hamilton's principle

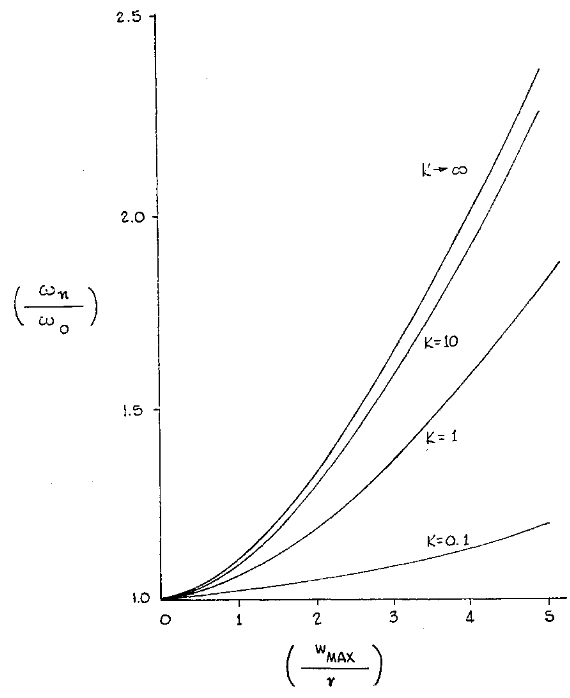

Fig. 1 Amplitude—frequency relationship; hinged ends.

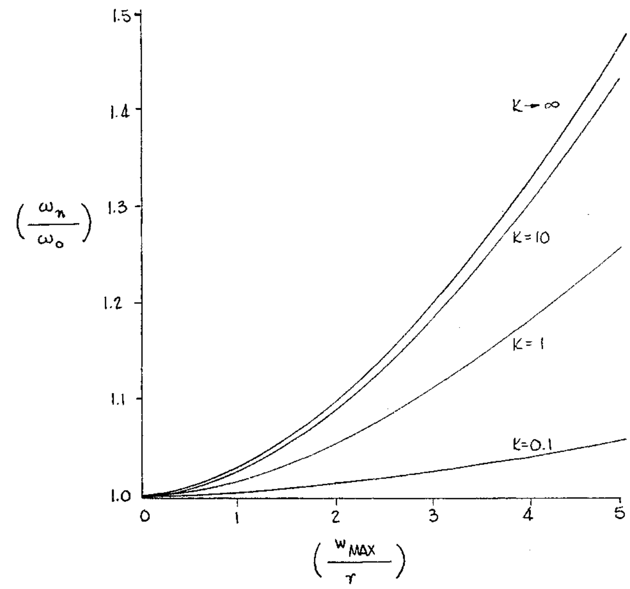

Fig. 2 Amplitude—frequency relationship; clamped ends.

leads to a set of nonlinear simultaneous differential equations. This set of equations is linear in h and i and by a suitable introduction of linear differential operators, h and i are eliminated yielding a single nonlinear differential equation in g. The approximate solution of this differential equation in g, by means of a perturbation technique, leads to

$$\left(\frac{\omega_n}{\omega_0}\right)^2 = \left\{1 + \left(\frac{n\pi r}{l}\right)^2\left(1 + \frac{EA}{D_Q}\right)\right\}^{-1} \times \left\{1 + \frac{3}{16}\alpha^2\left(\frac{K}{1+K}\right)\frac{[1 + (n\pi r/l)^2(1 + 2(EA/D_Q)]}{[1 + (n\pi r/l)^2(1 + (EA/D_Q)]}\right\} \qquad (2)$$

The validity of the approximate solution is most easily assessed by consideration of limiting cases. If transverse shear and rotatory inertia are neglected, while the effect of stretching is retained, Eq. (2) reduces to

$$(\omega_n/\omega_0)^2 = 1 + \tfrac{3}{16}\alpha^2[K/(1+K)] \qquad (3)$$

for finite axial restraint and to

$$(\omega_n/\omega_0)^2 = 1 + \tfrac{3}{16}\alpha^2 \qquad (4)$$

for the case of infinite axial restraint. In both of these limiting cases, the nonlinear differential equation for g can be solved exactly. For the case of infinite axial restraint, the solution is

$$(\omega_n/\omega_0)^2 = (\pi/2K_1)^2(1 + \alpha^2/4) \qquad (5)$$

For arbitrary axial restraint, the solution is

$$(\omega_n/\omega_0)^2 = (\pi/2K_1)^2\{1 + \alpha^2/4[K/(1+K)]\} \qquad (6)$$

The amplitude-frequency relationship is shown in Fig. 1. The results of the perturbation solution [Eq. (3)] are within approximately one percent of those obtained from the exact solution [Eq. (6)]. For a uniform homogeneous beam with clamped ends, the same procedure can be employed again where, for the first symmetrical mode,

$$w = g(t)[1 - \cos(2\pi x/l)]$$
$$u = h(t)[C_1x + C_2\sin(4\pi x/l)] \qquad (7)$$
$$\gamma = i(t)\sin(2\pi x/l)$$

The attendant amplitude-frequency relationship is shown in Fig. 2. Again, for the perturbation solution, the values of the frequency ratio are within approximately one percent of those obtained from the elliptic integral solution.

References

[1] Mayers, J. and Wrenn, B. G., "Combined Influence of Higher-Order Linear Effects and Nonlinear Effects on the Lateral Vibration Behavior of Solid and Sandwich Beams," SUDAER 208, Sept. 1964, Stanford Univ. Dept. of Aeronautics and Astronautics.

[2] Srinivasan, A. V., "Large Amplitude-Free Oscillations of Beams and Plates," *AIAA Journal*, Vol. 3, No. 10, Oct. 1965, pp. 1951–1953.

[3] Evensen, D. A., "Nonlinear Vibrations of Beams with Various Boundary Conditions," *AIAA Journal*, Vol. 6, No. 2, Feb. 1968, pp. 370–372.

[4] Ray, J. D. and Bert, C. W., "Nonlinear Vibrations of a Beam with Pinned Ends," *Transactions of the American Society of Mechanical Engineers* (*Journal of Engineering for Industry*), Nov 1969, pp. 997–1004.

[5] Woinowsky-Krieger, S., "The Effect of an Axial Force on the Vibration of Hinged Bars," *Journal of Applied Mechanics*, Vol. 17, No. 1, March 1950, pp. 35–36.

[6] Burgreen, D., "Free Vibrations of a Pin-Ended Column with Constant Distance Between the Pin Ends," *Journal of Applied Mechanics*, Vol. 18, No. 2, June 1951, pp. 135–139.

[7] Eringen, A. C., "On the Nonlinear Vibration of Elastic Bars," *Quarterly of Applied Mathematics*, Vol. 10, 1952, pp. 361–369.

[8] Chu, H. N. and Herrmann, G., "Influence of Large Amplitudes on Free Flexural Vibrations of Rectangular Elastic Plates," *Journal of Applied Mechanics*, Vol. 23, 1956, pp. 532–540.

[9] Chu, H. N., "Influence of Transverse Shear on Nonlinear Vibrations of Sandwich Beams with Honeycomb Cores," *Journal of the Aerospace Sciences*, Vol. 28, 1961, pp. 405–410.

[10] Young, D. and Felgar, R. P., "Table of Characteristic Functions Representing Normal Modes of Vibration of a Beam," Publication 4913, July 1949, Univ. of Texas, Austin, Texas.

[11] Felgar, R. P., "Formulas for Integrals Containing Characteristic Functions of a Vibrating Beam," Circular 14, 1950, Bureau of Engineering Research, Univ. of Texas, Austin, Texas.

[12] Herrmann, G., "Influence of Large Amplitude on Flexural Motions of Elastic Plates," TN 3578, 1956, National Advisory Committee for Aeronautics.

Shape and Surrounding Flowfield of a Drop in a High-Speed Gas Stream

A. A. Ranger*
Purdue University, Lafayette, Ind.
AND
J. A. Nicholls†
The University of Michigan, Ann Arbor, Mich.

Nomenclature

a = ellipse semimajor axis
b = ellipse semiminor axis
c = constant = $(a^2 - b^2)^{1/2}$
C_p = pressure coefficient = $(p - p_\infty)/(\frac{1}{2}\rho_\infty V_\infty^2)$
e = constant = $[1 - (b/a)^2]^{1/2}$
f = $c \sinh \xi$
k = constant = $e(1 - e^2)^{1/2} - \sin^{-1}e$
p = static pressure
r = polar coordinate (radial)
V = flowfield velocity
x = $c \sinh\xi \cos\eta$
y = $c \cosh\xi \sin\eta$
ζ = complex variable = $\xi + i\eta$
θ = polar coordinate (azimuthal)
Φ = velocity potential
ρ = fluid density

Subscripts

0 = droplet surface
∞ = undisturbed freestream conditions

Superscripts

$(\ )'$ = differentiation *wrt* ζ
$(\bar{\ })$ = complex conjugate

Received May 18, 1970; revision received June 10, 1970. The work reported here was conducted under NASA Contract NASr 54(07).

* Assistant Professor, School of Aeronautics, Astronautics, and Engineering Sciences. Member AIAA.

† Professor, Department of Aerospace Engineering. Associate Fellow AIAA.

Introduction

When a spherical liquid droplet is introduced into a convective gas stream it is observed to be flattened out in such a way as to present its largest dimension in a direction perpendicular to the oncoming flow.[1] The deformation that the drop undergoes is caused by the aerodynamic forces at the surface. The action of these external forces is opposed by the surface tension forces the inertial forces, and, to a lesser extent, by the viscous forces of the liquid. If the external forces are strong enough to overcome the internal restraining forces, the drop becomes unstable and disintegrates. The mechanism and speed of the ensuing breakup process depend on how much the aerodynamic pressure forces exceed the minimum value required to produce instability. If the pressure forces are just slightly larger than the minimum value necessary for fragmentation, the mechanism of breakup is the bag type.[2] On the other hand, if the aerodynamic forces far exceed the critical value, the disintegration appears to result from a boundary-layer stripping phenomenon.[3] It is the latter mechanism which has been observed to prevail in a high-speed gas stream.

The high-speed shattering of a droplet was first modeled analytically by G. I. Taylor[4] who assumed that the drop was squashed into a plano-convex lenticular shape before having its surface stripped away by the viscous shearing forces of the surrounding air stream. As a consequence of this assumption that the windward surface is spherical and the leeward one is planar, the diameter of the flattened drop was found to be approximately one and a half times larger than the initial diameter. However, an analysis of the photographic results of Ranger and Nicholls[5] indicates that the flattened drop has a maximum diameter that is appreciably greater than one and a half times the original, and that the shape of its windward surface is actually ellipsoidal. Unfortunately, it is impossible to ascertain from the photographs the shape of the leeward surface because it is completely obscured from view by a dense region of micromist being shed continuously from the droplet equator into its wake. The importance of these observations lies in the fact that the character of the flowfield surrounding a disintegrating droplet is quite different from that assumed by Taylor. In particular, the flow over the windward surface will be greatly influenced by the degree to which that surface deviates from being spherical. Thus, the purpose of the analysis that follows is to assess the influence of droplet shape on the velocity and pressure distributions over the windward surface of a drop in a high-speed gas stream. Flowfield calculations for this shape are not available in the literature.

Analysis

It has been established from experiment[5] that when a spherical liquid drop is introduced into a gas stream it responds to the attendant aerodynamic forces by deforming into a new shape closely resembling that of a planetary ellipsoid.‡ Naturally, any alteration in shape of the droplet will produce concurrent changes in the external flowfield around the drop, and vice versa, because the shape that the drop assumes and

‡ A planetary ellipsoid, which is also known as an oblate spheroid, is the body generated by rotating an ellipse about its minor axis.